GEOLOGIJA. 2006. Vol. 55. P. 24–36


*Ekonominė geologija • Economic Geology • Экономическая геология*

# Modelling of radionuclide transport in crystalline basement for demonstration of spent nuclear fuel disposal feasibility (case of South-eastern Lithuania)

**Vaidotė Jakimavičiūtė-Maselienė,**

**Jonas Mažeika,**

**Rimantas Petrošius**

Jakimavičiūtė-Maselienė V, Mažeika J., Petrošius R. Modelling of radionuclide transport in crystalline basement for demonstration of spent nuclear fuel disposal feasibility (case of South-eastern Lithuania). *Geologija.* 2006. Vol. 55. P. 24–36. ISSN 1392-110X

The Strategy of Radioactive Waste Management of Lithuania provides for evaluating the possibilities of disposal in a deep geological repository of spent nuclear fuel and long-lived radioactive waste originated from the Ignalina NPP. The initial feasibility studies performed in Lithuania during 2001–2004 focus on screening all potentially prospective rock types as a host medium for a repository. Since most information is available on crystalline basement and sedimentary cover of South-eastern Lithuania, this host medium was selected for model case studies. Taking into account the main assumptions (the canister defect scenario proposed by Swedish experts and evaluated by LEI experts) groundwater flow and radionuclide (iodine-129 as a mobile and long-lived one) transport modeling using FEFLOW computer code was performed to model the domain (approximately a 0.8 km long, 0.6 km wide and 0.52 km thick far-field block) of South-eastern Lithuania. The model domain comprises a Proterozoic–Archaean aquifer with an overlaying aquifer system of sedimentary cover. The upward groundwater flow through a defected canister located in a tectonically damaged zone was conservatively generated. The main results of calculations are the following: in case of upward groundwater flow, the maximum activity concentration of I-129 in the single longitudinal tectonic fracture above the defected canister will not exceed $10^{-4}$ Bq/l, and in the active water exchange zone it is close to $10^{-7}$ Bq/l. These figures show that doses obtained by a human recipient via the aquatic pathway should be below the dose limit (1 mSv/y). Location of the model domain in South-eastern Lithuania does not mean any reference to the site for a deep geological repository.

**Key words:** spent nuclear fuel, geological repository, crystalline basement, groundwater, finite elements model

Received 06 February 2006, accepted 25 May 2006

Vaidotė Jakimavičiūtė-Maselienė, Jonas Mažeika, Rimantas Petrošius, Institute of Geology and Geography, T. Ševčenkos 13, LT-03223 Vilnius, Lithuania. E-mail: jakimaviciute@geo.lt, mazeika@geo.lt, petrosius@geo.lt

## INTRODUCTION

During operation of the Ignalina NPP (INPP) spent nuclear fuel (SNF) is produced. Since May 1999, SNF, after being stored in water ponds inside the NPP buildings, was removed from there, loaded into CASTOR RBMK-1500 or CONSTOR RBMK-1500 casks and transported to an interim storage facility in the industrial area of the NPP. SNF can be stored in these casks for at least 50 years. Due to the danger of exposure arising from the long-lived radionuclides to the humans and environment, SNF is not allowed to be disposed of in near-surface repositories (IAEA…, 1985; Deep…, 1998).

Several alternatives related to safe management and disposal of SNF are being analysed for the future: a deep geological repository for SNF and long-lived radioactive wastes in any SNF-generating country, a regional repository constructed by joint efforts of several countries that generate (or not) SNF, disposal of SNF in other countries, and the possibility of extending the storage period in an interim storage for up to 100 and more years.

There is an international consensus that high-level and long-lived radioactive waste, first of all SNF, is best disposed of in deep geological repositories using a system of engineered and natural barriers (The scientific…, 1995). "In the current climate geological repositories have come to be viewed not as one option among many for completing the nuclear fuel cycle, but as the only sustainable solution achievable in the near term" (*Mohamed ElBaradei, Director General, International Atomic Energy Agency, Stockholm 08 12 2003*). It is a common opinion that there are few environments for which evidence of their stability over hundreds of thousands of years exists. Modern technology enables assessing old deep geological formations as the most obvious candidate environments.

No geological repository is in operation yet, however, repository projects in Finland, Sweden and the USA have advanced to a stage at which decisions can be made to begin construction (Deep…, 1998). Crystalline basement rock is regarded as the best investigated host medium for SNF disposal worldwide. Since most information regarding deep geological media in Lithuania is available on the crystalline basement of South-eastern Lithuania, this host medium with the overlaying sedimentary cover was selected for the model case studies (Concept…, 2005; Generic…, 2005; Suitability…, 2005).

Taking into account the main assumptions (canister defect scenario evaluated by LEI experts), groundwater flow and radionuclide (iodine-129 as a mobile and long-lived one) transport modeling using FEFLOW computer code was performed for a model domain located in South-eastern Lithuania. It has been conservatively taken that groundwater from the host medium through two perpendicular fractures discharges into the upper aquifer system in a significant part of the model domain.

Location of this conservatively complicated model domain in a certain territory of Lithuania does not mean any reference to the site as a deep geological repository. Location of the model domain in a particular area has a demonstrative value in order to show the possible environmental impact of a deep geological repository constructed in this area.

## OUTLINE OF THE PROBLEM OF SPENT NUCLEAR FUEL

The expected total amount of SNF produced by the INPP until 2010 is 21941 fuel assemblies or about 2436 tons of SNF (Generic…, 2002). The radionuclide inventory in the SNF will consist of actinides, fission products, and many activation radionuclides. Most of radionuclides lie embedded in the fuel matrix of uranium dioxide for a very long time. Some of the fission products, including iodine-129, are relatively mobile.

Repositories for the disposal of SNF and high-level waste generally rely on a multi-barrier system to isolate the waste from the biosphere. The multi-barrier system usually comprises a natural geological barrier and an engineered barrier system (Vieno, 1994). The host rock types currently under investigation are salts (in either salt domes or bedded formations), granite or similar crystalline rocks, argillaceous rocks, tuff and basalt. The best investigated host rocks to date are crystalline rocks.

The Finnish government and local population were the first to recently approve a preferred site for SNF disposal in the granite at Olkiluoto on the Baltic Coast. Sweden has focused onto two granite areas. Other countries that have considered granite-siting options include France, Switzerland, Spain and Canada.

The most developed Swedish concept KBS-3 for a deep geological repository involves encapsulating the fuel in copper canisters with cast iron inserts, embedding each canister vertically or horizontally and surrounding them with bentonite clay at a depth of about 500 m in the crystalline basement (Summary…, 2004).

Plans for the final disposal of SNF in Finland are based on the same KBS-3 concept. The concept comprises horizontal tunnels in the crystalline rock at a depth of most likely 500 m, with vertical holes drilled in the floors.

The overview of the geological structure and composition of the sedimentary cover and crystalline basement of Lithuania was carried out in 2001–2002 starting the feasibility studies aimed to assess the whole territory of Lithuania in terms of suitability for a deep geological repository. Several major candidates of geological media in Lithuania (clayey formations, rock salt and anhydrite formations, crystalline basement rocks) were selected for future considerations.

As a result of the overview, four clayey formations perspective as a host rock were distinguished in the sedimentary cover of Lithuania. They are represented by the Lower Cambrian, Lower Silurian, Middle Devonian

and the Lower Triassic sequences. The most perspective from clayey formations were assumed to be the Lower Cambrian and Lower Triassic sequences. The Lower Cambrian Baltija Formation occurs only in the eastern part of Lithuania (proximity to the INPP region). The top of the succession occurs at a depth of 200–1000 m, dipping to the NW. The thickness reaches 115 m in the easternmost part, decreasing to the west to 50 m (Paškevičius, 1994). The Lower Triassic sequence occurs only in southwest Lithuania (quite far from the INPP). The shallow depth of occurrence, rather homogeneous lithological composition, sufficient thickness, favourable mechanical properties of Lower Triassic rock allowed considering it as one of the most promising clayey for-

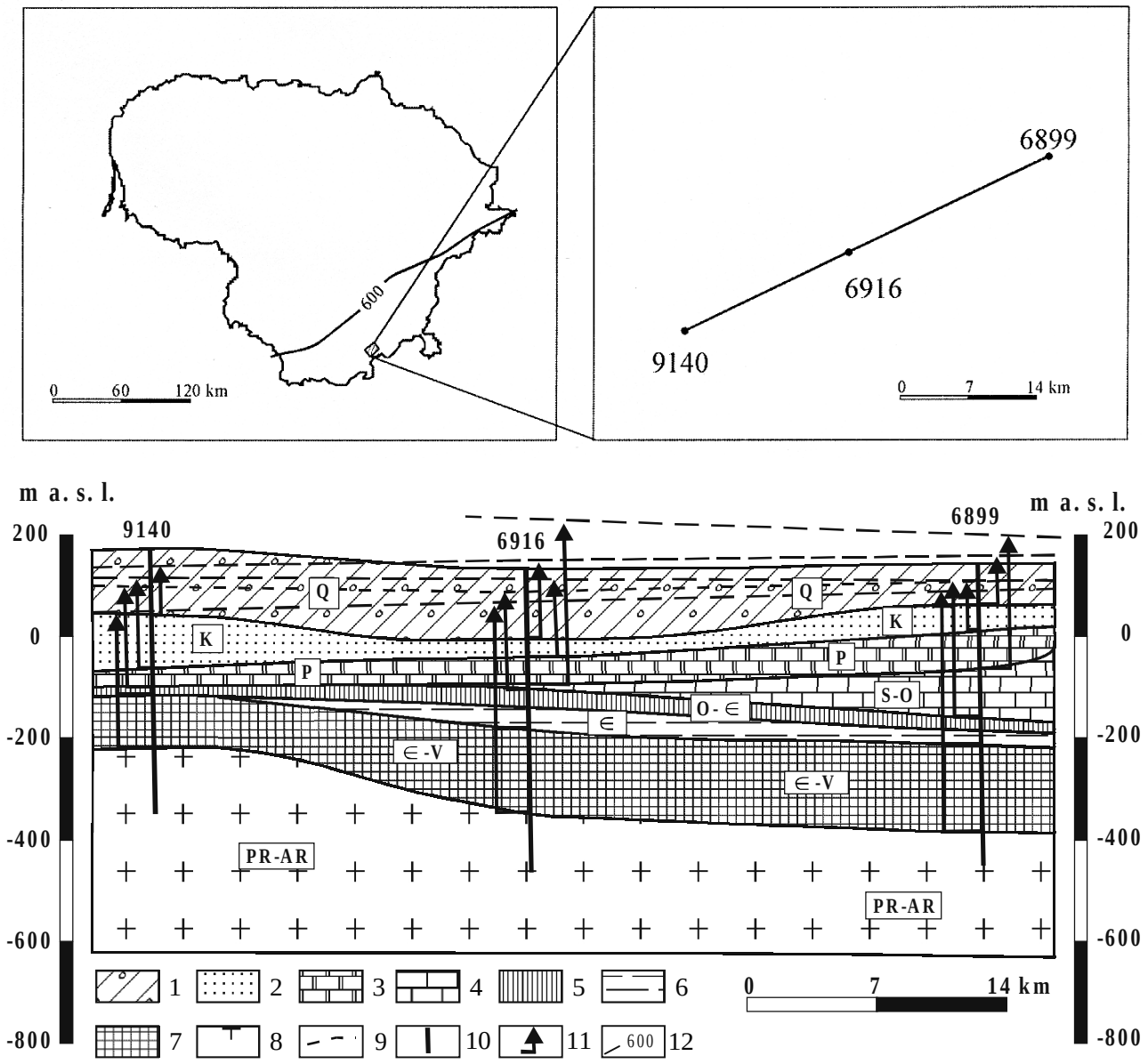


**Fig. 1.** Study area location and hydrogeological cross-section: *1* – Quaternary deposits (glacial till, silt and various sands), *2* – Cretaceous (sandy deposits, silt and chalk), *3* – Permian (limestone and sandstone), *4* – Silurian – Upper-Middle Ordovician (limestone and clay), *5* – Lower Ordovician – Cambrian (limestone, clayey limestone and sandstone), *6* – Lower Cambrian (argillite, sandstone and clay), *7* – Cambrian–Vendian (sandstone and argillite), *8* – Proterozoic–Archaean (crystalline rocks), *9* – groundwater level, *10* – well, *11* – hydraulic head, *12* – isoline of crystalline basement depth of 600 m from Earth surface

**1 pav.** Tyrimų plotas ir jo hidrogeologinis pjūvis: *1* – kvartero nuogulos (moreninis priemolis, aleuritas ir įvairus smėlis), *2* – kreida (smėlingos nuogulos ir kreida), *3* – permas (klintis ir smiltainis), *4* – silūras–viršutinis ir vidurinis ordovikas (klintis ir molis), *5* – apatinis ordovikas–kambras (klintis, molinga klintis ir smiltainis), *6* – apatinis kambras (argilitas, smiltainis ir molis), *7* – kambras–vendas (smiltainis ir argilitas), *8* – proterozojus–archėjus (kristalinės uolienos), *9* – požeminio vandens lygis, *10* – gręžinys, *11* – hidraulinis spūdis, *12* – kristalinio pamato 600 m gylio izolinija

mations in terms of SNF disposal. Other clayey formations (Lower Silurian and Middle Devonian) were considered to be less perspective as a host rock.

The Upper Permian (Zechstein) anhydrite and rock salt of the Prieglius Formation occurred at a depth of 150–790 m in a more than 12 000 km$^2$ area of South and Southwest Lithuania. Studies of well logs of areas drilled with no core sampling have showed that the suggested salt domes in fact are anhydrite and gypsum bodies. Therefore, the Usėnai dome was considered as the only salt body known in Lithuania. After feasibility studies it was concluded that rock salt media could not be regarded as a highly potential alternative for SNF disposal (Suitability…, 2005).

The best prospects of the crystalline basement appeared to be related to South-eastern Lithuania where the basement rocks are overlain by only a 200–300 m thick sedimentary cover, while the central and western parts of Lithuania are devoid of a deep burial crystalline basement. The extensive geological information available on South-eastern Lithuania makes the crystalline basement option very reasonable for future studies (Suitability…, 2005).

## HYDROGEOLOGICAL SETTING

The hydrogeological framework of the southern Lithuanian region was based on the information summarized in recent geoscientific generalizations (Иодказис, 1989; Mokrik, 2003; Dundulis et al., 2004; Mikšys, 2004; Suitability…, 2005).

In order to construct a model domain (an approximately 0.8 km long, 0.6 km wide and 0.52 km thick far-field block), a well characterized by deep drilling (boreholes 9140, 6916, 6899) hydrogeological cross-section 43 km long in South-eastern Lithuania was selected (Fig. 1).

Table 1. **Hydrogeological parameters selected for different zones (numbers in brackets) of modelling domain in the southern part of Lithuania (Adam et al., 1985; Dundulis et al., 2004; Mikšys, 2004; Suitability…, 2005; Иодказис, 1989)**

1 lentelė. **Radionuklidų pernašos vandeninguosiuose horizontuose Pietų Lietuvos sąlygomis skirtingų zonų modelio (skaičiai skliaustuose) hidrogeologiniai parametrai (pagal Adam et al., 1985; Dundulis et al., 2004; Mikšys, 2004; Suitability…, 2005; Иодказис, 1989)**

| No. | Geological formation | Lithological description (prevailing) | Thickness, m | Hydraulic conductivity, $10^{-4}$ m/s | Porosity | Density, kg/m$^3$ | Henry sorption for $^{129}$I | Longitudinal dispersivity, m | Transverse dispersivity, m |
|---|---|---|---|---|---|---|---|---|---|
| 1 | Quaternary | Loam (1, 3), sand (2) | 20 | 0.1 (1, 3), 7.5 (2) | 0.25 (1, 3), 0.41 (2) | 2000 (1, 3), 1700 (2) | 2 (1, 3), 1.7 (2) | 0.01 (1, 3), 0.5 (2) | 0.001 (1, 3), 0.05 (2) |
| 2 | | Sand (1), loam (2, 3), | 20 | 7.5 (1), 0.1 (2, 3) | 0.41 (1), 0.25 (2, 3) | 1700 (1), 2000 (2, 3) | 1.7 (1), 2 (2, 3) | 0.5 (1), 0.01 (2, 3) | 0.05 (1), 0.001 (2, 3) |
| 3 | | Silt (1), sand (2), loam (3) | 20 | 0.05 (1), 2.5 (2), 0.005 (3) | 0.4 (1), 0.41 (2), 0.25 (3) | 2007 (1), 1700 (2), 2000 (3) | 2.01 (1), 1.7 (2), 2 (3) | 0.01 (1, 3), 0.5 (2) | 0.001 (1, 3), 0.05 (2) |
| 4 | | Loam (1-3) | 20 | 0.005 (1-3) | 0.25 (1-3) | 2000 (1-3) | 2 (1-3) | 0.01 (1-3) | 0.001 (1-3) |
| 5 | | Sand (1, 2), loam (3) | 20 | 2.5 (1, 2), 0.005 (3) | 0.41 (1, 2), 0.25 (3) | 1700 (1, 2), 2000 (3) | 1.7 (1, 2), 2 (3) | 0.5 (1, 2), 0.01 (3) | 0.05 (1, 2), 0.001 (3) |
| 6 | Cretaceous | Chalk (1, 3), silt (2) | 20 | 0.17 (1, 3), 0.05 (2) | 0.48 (1, 3), 0.41 (2) | 2100 (1, 3), 2007 (2) | 2.1 (1, 3), 2.01 (2) | 5 (1, 3), 0.01 (2) | 0.5 (1, 3), 0.001 (2) |
| 7 | | Chalk (1), silt (2), | 20 | 0.17 (1), 0.05 (2), | 0.48 (1), 0.41 (2), | 2100 (1), 2007 (2), | 2.1 (1), 2.01 (2), | 5 (1), 0.01 (2), | 0.5 (1), 0.001 (2), |
| 8 | | fine-grained sand (3) | 20 | 0.6 (3) | 0.35 (3) | 1600 (3) | 1.6 (3) | 0.5 (3) | 0.05 (3) |
| 9 | | Medium-grained sand (1, 2), fine-grained sand (3) | 20 | 2.5 (1, 2), 0.6 (3) | 0.35 (1-3) | 1700 (1, 2), 1600 (3) | 1.7 (1, 2), 1.6 (3) | 0.5 (1-3) | 0.05 (1-3) |
| 10 | | Medium-grained sand (1, 2), chalk (3) | 20 | 2.5 (1, 2), 0.17 (3) | 0.35 (1, 2), 0.48 (3) | 1700 (1, 2), 2100 (3) | 1.7 (1, 2), 2.1 (3) | 0.5 (1, 2), 5 (3) | 0.05 (1, 2), 0.5 (3) |
| 11 | Permian | Limestone (1, 3), clayey limestone (2) | 25 | $1.2\times10^{-5}$ (1, 3), $7\times10^{-8}$ (2) | 0.13 (1-3) | 2600 (1-3) | 2.6 (1-3) | 5 (1, 3), 3 (2) | 0.5 (1, 3), 3 (2) |

**Table 1 (continued)**
**1 lentelės tęsinys**

| No. | Geological formation | Lithological description (prevailing) | Thick-ness, m | Hydraulic conductivity, $10^{-4}$ m/s | Porosity | Density, kg/m$^3$ | Henry sorption for $^{129}$I | Longitudinal dispersivity, m | Transverse dispersivity, m |
|---|---|---|---|---|---|---|---|---|---|
| 12 | | Sandstone (1), clayey limestone (2), limestone (3) | 25 | 2 (1), $7\times10^{-8}$ (2), $1.2\times10^{-5}$ (13) | 0.05 (1), 0.13 (2, 3) | 2700 (1), 2600 (2, 3) | 2.7 (1), 2.6 (2, 3) | | |
| 13 | Silurian–Ordovician | Limestone (1, 2), clay (3) | 10 | $7\times10^{-6}$ (1), $1.2\times10^{-5}$ (2), $1\times10^{-4}$ (3) | 0.13 (1, 2), 0.5 (3) | 2600 (1, 2), 2700 (3) | 2.6 (1, 2), 2.7 (3) | 5 (1, 2), 0 (3) | 0.5 (1, 2), 0 (3) |
| 14 | | Limestone (1-3) | 10 | $7\times10^{-6}$ (1), $1.2\times10^{-5}$ (2,3) | 0.13 (1-3) | 2600 (1-3) | 2.6 (1-3) | 5 (1-3) | 0.5 (1-3) |
| 15 | Ordovician–Cambrian | Sandstone (1), clayey limestone (2), limestone (3) | 10 | 2 (1), $7\times10^{-6}$ (2), $1.2\times10^{-5}$ (3) | 0.05 (1), 0.13 (2, 3) | | | 5 (1, 3), 3 (2) | 0.5 (1, 3), 0.3 (2) |
| 16 | | | 10 | | | | | | |
| 17 | Cambrian | Argillite (1), sandstone (2, 3) | 10 | $1\times10^{-7}$ (1), 1 (2), 2 (3) | 0.2 (1), 0.05 (2, 3) | 2650 (1), 2600 (2, 3) | 2.65 (1), 2.6 (2, 3) | 0.01 (1), 5 (2, 3) | 0.001 (1), 0.5 (2, 3) |
| 18 | | Argillite (1), sandstone (2), clay (3) | 10 | $1\times10^{-7}$ (1), 1 (2), $1\times10^{-4}$ (3) | 0.2 (1), 0.05 (2), 0.28 (3) | 2650 (1), 2600 (2), 2700 (3) | 2.65 (1), 2.6 (2), 2.7 (3) | 0.01 (1), 5 (2), 0 (3) | 0.001 (1), 0.5 (2), 0 (3) |
| 19 | Cambrian–Vendian | Sandstone (1, 3), argillite (2) | 20 | 2 (1, 3), $1\times10^{-7}$ (2) | 0.05 (1, 3), 0.2 (2) | 2600 (1, 3), 2650 (2) | 2.6 (1, 3), 2.65 (2) | 5 (1, 3), 0.01 (2) | 0.5 (1, 3), 0.001 (2) |
| 20 | | | 20 | | | | | | |
| 21 | | | 20 | | | | | | |
| 22 | | | 20 | | | | | | |
| 23 | | | 20 | | | | | 0.01 (1, 2), 5 (3) | 0.001 (1, 2), 0.5 (3) |
| 24 | Proterozoic–Archaean | Milonite (1), sandstone (2), gravellite (3) | 10 | $2\times10^{-4}$ (1), 0.1 (2, 3) | 0.004 (1), 0.005 (2), 0.006 (3) | 2380 (1-3) | 2.38 (1-3) | 0.01 (1, 3), 0.1 (2) | 0.001 (1, 3), 0.01 (2) |
| 25 | | Epidozite (1), breccia (2), granite-gneisses (3) | 20 | $1\times10^{-8}$ (1), $2\times10^{-5}$ (2), $2\times10^{-8}$ (3) | 0.0007 (1), 0.00116 (2), 0.00075 (3) | 2900 (1), 2500 (2), 2650 (3) | 2.9 (1), 2.5 (2), 2.65 (3) | 5 (1-3) | 0.5 (1-3) |
| 26 | | | 20 | | | | | | |
| 27 | | Epidozite (1), plagiogneisses (2), granite-gneisses (3) | 20 | $1\times10^{-8}$ (1), $1.6\times10^{-8}$ (2), $2\times10^{-8}$ (3) | 0.0007 (1), 0.00075 (2,3) | 2900 (1), 2640 (2), 2650 (3) | 2.9 (1), 2.64 (2), 2.65 (3) | | |
| 28 | | Granite-gneisses (1,3) plagiogneisses (2) | 20 | $2\times10^{-8}$ (1, 3), $1.6\times10^{-8}$ (2) | 0.00075 (1-3) | 2650 (1, 3), 2640 (2) | 2.65 (1, 3), 2.64 (2) | | |
| 29 | | | 20 | | | | | | |

Table 2. **Parameters of the two perpendicular single fractures representing tectonic fault zone (Adam et al., 1985)**

2 lentelė. **Dviejų statmenai besikertančių tektoninių lūžių parametrai (pagal Adam et al., 1985)**

| Parameters | Crystalline rocks (PR-AR) | Sandstone (CM-V) |
|---|---|---|
| Thickness, m | 1 | 1 |
| Hydraulic conductivity, $10^{-4}$ m/s | 60 | 5 |
| Porosity | 0.3 | 0.26 |
| Longitudinal dispersivity, m | 0.01 | 5 |
| Transverse dispersivity, m | 0.001 | 0.5 |
| Henry sorption for $^{129}$I | 2 | 1.8 |
| Rock density, kg/m$^3$ | 2000 | 1800 |

The site-specific and generic parameters of this section are given in Tables 1 and 2.

Quaternary deposits (glacial till, silt and various sands) in the area of the model domain occur at the land surface and form the uppermost part of the geological succession. The total thickness of these deposits varies from 80 to 143 m (average 119 m). There are a shallow groundwater layer and several semi-confined aquifers in the Quaternary cover. The piezometric level and hydraulic properties of Quaternary aquifers are different and depend on the complexity of the geological structure. For modelling purposes, all Quaternary aquifers are regarded as a unified aquifer system (Suitability…, 2005).

The Cretaceous aquifer consists of chalk, silt and sand. The top of the aquifer dips from the altitude of

61 m a.s.l. to the -10 m b.s.l. The thickness of the aquifer varies from 30 to 105 m. The hydraulic head of the aquifer varies between the altitudes of 150 and 155 m a.s.l.

The Permian aquifer consists of fractured limestone and sandstone. The top of the aquifer occurs at a depth from of 141 m to 244 m. It dips to the west and southwest. The hydraulic head occurs between the altitudes of 160 and 210 m a.s.l.

The Silurian – Upper and Middle Ordovician aquifer system occurs over the studied area except the southernmost edge. It consists of limestone and clay. The top of the aquifer occurs at a depth of 204 m to 277 m. It dips to the west and northwest. The hydraulic head occurs at an altitude 150 m a.s.l.

The Lower Ordovician – Cambrian aquifer system consists of limestone, clayey limestone and sandstone. The altitude of the aquifer top varies, from -150 m to -210 m b. s. l. It dips to the west. The hydraulic head varies between the altitudes of 80 and 150 m a. s. l.

The Lower Cambrian aquitard occurs in the northern and northeastern parts of the area. It consists of argillite, sandstone and clay. The depth of the layer varies from 259 to 287 m. The altitudes of occurrence range between -140 m in the southern and -210 m b.s.l. in the northwestern part of the area.

The Cambrian – Vendian aquifer system consists of sandstone and argillite. It occurs in all the area at a depth between 300 and 450 m. The aquifer is dipping to the east. Its thickness reaches 100 m in the eastern part of the study area. The aquifer has a strong hydraulic connection with the underlying Protherozoic–Archaean aquifer. Therefore, the hydraulic heads of these two systems are similar. They are about 20 m a. s. l. in the south-western part and more than 110 m a. s. l. in the northeast.

The Proterozoic–Archaean aquifer lies over the study area. It consists of fractured crystalline rocks and occurs at a depth from 300 m to more than 600 m. The basement rocks are overlain by sediments deposited at different stages of the basin evolution. Accordingly, the crystalline rocks were exposed to denudation and weathering for different time intervals under various climatic conditions. Commonly, the upper part of the basement is weathered. The composition of the weathered crust varies significantly, depending on the composition of the basement rocks and physical-chemical exogenic conditions. Groundwater is accumulated in weathering and tectonic fractures. The permeability of the aquifer could reach 50 $m^2$/d, and the specific yield could be between 0.25 and 0.35 l/s (Suitability…, 2005).

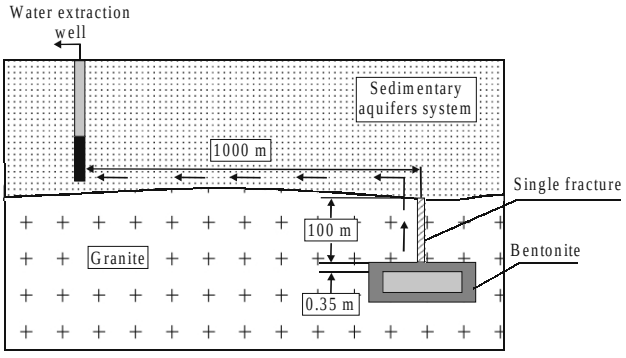


**Fig. 2.** Conceptual model of radionuclide transport from defected canister disposed of in crystalline basement (not to scale) (Generic…, 2005)

**2 pav.** Radionuklidų pernašos vandeninguosiuose horizontuose iš suirusio kanistro, patalpinto kristalinių uolienų pamate, konceptualus modelis (be mastelio) (Generic…, 2005)

## CONCEPTUAL MODEL

According to the MLH variant of the Swedish KBS-3H concept (Medium Long Hole) where the canisters are proposed to deposit in a 150–500 m long deposition hole on both sides of the transport tunnel, the evolution of one canister was considered (KBS-3, 2004).

The copper canister selected as a prototype for SNF from the Ignalina NPP is composed of two components: an outer corrosion protective shell of copper and a cast iron insert with channels for the fuel half-assemblies in order to improve the mechanical strength. One canister can hold 32 RBMK-1500 fuel half-assemblies; for Lithuanian disposal purposes about 1400 canisters should be employed. A copper canister with the 50 mm thick wall should be made of oxygen-free copper with a low phosphorus content. The canister insert is cast of steel and will have a minimum wall thickness of 50 mm. The preliminary data for the reference canister are 1050 mm in diameter and 4070 mm in length (Brazauskaitė, Poškas, 2005).

The chemical evolution of a damaged canister differs radically from that of an intact canister. Water intruding into a defected canister gives rise to several important chemical reactions, namely: corrosion of the cast iron insert, corrosion of the fuel claddings and other metallic parts, release of radionuclides in these parts, dissolution of the fuel matrix with release of radionuclides.

Following several cases considered in detail in (Deep…, 1998) and referenced in (Generic…, 2005), the most conservative case was selected in this study, assuming that SNF is completely dissolved when a continuous water pathway is created (instant release fraction 100%).

A very simple conceptual model of radionuclide transport in the repository system including far-field aquifers is presented in Fig. 2.

This conceptual model was derived from hydrogeological conditions demonstrated in the hydrogeological section (Fig. 1).

It is conservatively taken that the canister is located in the tectonic fault zone of the crystalline basement. In the final model, the tectonic fault zone is comprised of two perpendicular single fractures. The groundwater washing the canister discharges into the upper aquifers. To enhance the hydrodynamic effect, it is assumed that

a productive well (yield value is 3000 $m^3$/day) is installed 363 m from the canister in the Ordovician–Cambrian aquifer (sandstone).

The migration of radionuclides from a repository toward the far-field aquifers and eventually toward the surface (or biosphere) can only start when the canister containing SNF has been defected, the SNF has been dissolved by water and radionuclides have been transported away from the container through the engineered barriers surrounding them. In this study, the time for the mentioned processes is assumed 200 000 years (Generic…, 2005).

The major important radionuclide migration mechanisms to be taken into account: advection in saturated zone, molecular diffusion, hydrodynamic dispersion and retardation by interactions with the solid phase (De Marsily et al., 2005; Krishnamoorthy, Nair, 1994). There are many types of possible interactions, the most common being adsorption, particularly in the case of small particles (silt, clay, etc.) (Chang, Cho, 1984; Lucero, 1998; Vilks et al., 1998).

The main considered radionuclide is iodine-129, whose inventory per canister in the model case study assumed to be the same as in the Swedish BWR fuel (2.31E ± 09 Bq, I-129 half life 1.57E ± 07 years). The estimated I-129 release rate through engineered barriers to far-field was taken from the study (Generic…, 2005) as the input function for 3D modeling of radionuclide transport in far-field.

## COMPUTER CODE AND NUMERICAL MODEL

The continuum approach is the standard to describe the fundamental processes of flow and transport in porous media (Ferziger, Peric, 1996). The assumption of continuum implies that the main physical properties (velocity, pressure, concentration, etc.) are continuously distributed in space and thus exist for any infinitely small material point. In most porous-media, the problems of mass, motion and energy-related quantities can neither be measured nor solved at a microscopic level due to the geometric complexity of real geologic media. These difficulties are resolved by a transformation to the macroscopic level by averaging over volumes leading to measurable and solvable quantities for which the continuum assumption is then invoked. The related macroscopic equations are solved by numerical methods (Baker, 1998; Chavent, Jaffe, 1986). Popular and powerful strategy is the finite element and finite volume method. Both methods have the same mathematical basis with weighted-integral formulation of the governing balance equations (Ferziger, Peric, 1996).

The finite element modeling has broad applications in various disciplines, including petroleum engineering (hydrocarbon-gas injection and recycling in gas-condensate reservoirs), contaminant hydrogeology and geochemical engineering (contamination of groundwater aquifers and radioactive waste management in the subsurface).

The numerical model used in this study is based on the three-dimensional finite-element code FEFLOW 5.0, which allows modeling groundwater flow and contaminant transport in a layered three-dimensional system taking into account the fracture phenomenon. The simulation system based on the FEFLOW code models flow and contaminant mass processes as coupled or separate phenomena (Diersch, 2002). It is based on the physical conservation principles for mass, chemical species, linear momentum and energy in a transient and three-dimensional numerical analysis.

For three-dimensional (3D) and two-dimensional (2D) – vertical and axisymmetric, respectively – processes, the representative model general equations are as follows *(i, j = 1,2,3)*:

$$S_0 \frac{\partial h}{\partial t} + \frac{\partial q_i^f}{\partial x_j} = Q_\rho + Q_{EB}(C,T), \quad (1)$$

$$q_i^f = -K_{ij} f_\mu \left( \frac{\partial h}{\partial x_j} + \frac{\rho^f - \rho_0^f}{\rho_0^f} e_j \right), \quad (2)$$

$$\varepsilon R_d \frac{\partial C}{\partial t} + q_i^f \frac{\partial C}{\partial x_i} - \frac{\partial}{\partial x_i}\left( D_{ij} \frac{\partial C}{\partial x_j} \right) + \left( \varepsilon R \vartheta + Q_p \right) C = Q_C, \quad (3)$$

with the constitutive equations:

$$\rho^f = \rho_0^f \left[ 1 + \frac{\bar{a}}{(C_s - C_0)} (C - C_0) \right], \; h = \frac{p^f}{\rho_0^f g} + x_i, \; K_{ij} = \frac{k_{ij} \rho_0^f g}{\mu_0^f},$$

$$\bar{a} = \left[ \rho^f (C_s) - \rho_0^f \right] / \rho_0^f,$$

$$f_\mu = \frac{\mu_0^f}{\mu^f (C,T)} = \frac{1 + 1.85\omega_{(C=C_0)} - 4.1\omega^2_{(C=C_0)} + 44.5\omega^3_{(C=C_0)}}{1 + 1.85\omega - 4.1\omega^2 + 44.5\omega^3} \cdot$$

$$\cdot \frac{1 + 0.7063\varsigma - 0.04832\varsigma^3}{1 + 0.7063\varsigma_{(T=T_0)} - 0.04832\varsigma^3_{(T=T_0)}},$$

$$\varsigma = \frac{(T - 150)}{100}, \; \omega = \frac{C}{\rho^f}, \; D_{ij} = (\varepsilon D_d + \beta_T V_q^f)\delta_{ij} + (\beta_L - \beta_T) \frac{q_i^f q_j^f}{V_q^f},$$

$$R = 1 + \tfrac{(1-\varepsilon)}{\varepsilon} \chi(C), \; R_d = 1 + \frac{(1-\varepsilon)}{\varepsilon} \frac{\left[ \chi(C) \cdot C \right]}{\partial C},$$

which are to be solved for the three primary variables ($h$ – hydraulic head; $q_i^f$ – Darcy velocity vector of fluid; $C$ – concentration of the chemical component or activity concentration of the radionuclide).

The main governing parameters are: $\rho^f, \rho_0^f$ – fluid and reference fluid density, respectively; $\rho^S$ – solid density; $S_0$ – specific storage coefficient (compressibility); $K_{ij}$ – tensor of hydraulic conductivity; $e_j$ – gravitational unit vector; $f_\mu$ – constitutive viscosity relation function; $Q_{EB}$ – term of extended Boussinesq approximation; $R$ – specific retardation factor; $R_d$ – derivative term of retardation; $D_{ij}$ – tensor of hydrodynamic dispersion;

$\delta_{ij}$ – Kronecker tensor; $\upsilon$ – decay rate ($\lambda$ is the most conventional designation for the radioactive decay rate); $\varepsilon$ – porosity; $Q_x$ – source/sink function of fluid ($x = \rho$) and contaminant mass ($x = C$); $\bar{a}$ – fluid density difference ratio; $\overline{\beta}$ – fluid expansion coefficient; $C_0$, $T_0$ – reference values for concentration and temperature, respectively; $C_s$ – maximum concentration; $p^f$ – fluid pressure; $g$ – gravitational acceleration; $k_{ij}$ – tensor of permeability; $\mu^f, \mu_0^f$ – dynamic viscosity and its reference value, respectively, of fluid; $\zeta$ – normalized temperature; $\omega$ – mass fraction; $D_d$ – molecular diffusion coefficient of fluid; $V_q^f - \sqrt{q_i^f q_i^f}$ – absolute Darcy fluid flux; $\beta_L$, $\beta_T$ – longitudinal and transverse dispersivity, respectively, of chemical species; $\chi(C)$ – concentration-dependent adsorption function.

The relationships of retardation $R$ and $R_d$ can be summarized for the different adsorption laws as follows (Diersch, 2002):

$$\text{Henry isotherm: } R = \varepsilon(1-\varepsilon)K, R_d = \varepsilon + (1-\varepsilon)K, \quad (4)$$

where $K$ is the Henry sorption coefficient.

The Henry sorption coefficient of the radionuclides is calculated as

$$K = k_d \rho^s, \quad (5)$$

where $k_d$ is the distribution coefficient for a particular radionuclide, $m^3/kg$; $\rho^S$ is the density of solid, $kg/m^3$.

From general equations, the horizontal model equations which differ in confined and unconfined conditions and convective and divergence forms of contaminant transport equations are derived. The governing model equations have to be supplemented by initial, boundary, and constraint conditions (Diersch, 2002).

A rather complicated but conservative in terms of groundwater flow formulation numerical model was worked out based on the conceptual model (Table 3).

Once calibrated, the model was used to predict radionuclide transport in groundwater and its potential effect on the environment. The numerical model is constructed in such a way as to imitate a greater migration of radionuclides to aquifers than it could be possible under the chosen geological conditions. The defected canister is installed in the top part of the crystalline basement in the crossing point of two perpendicular single fractures, though following the conceptual design it should be at a depth of 100 m.

Table 3. **Features of the numerical model of radionuclide transport for the domain of Southern Lithuania**
3 lentelė. **Radionuklidų pernašos vandeninguosiuose horizontuose Pietų Lietuvos sąlygomis skaitmeninio modelio savybės**

| | | | |
|---|---|---|---|
| Problem class | Combined flow and mass transport model | Vertical exaggeration | 1:1 |
| Time class | Transient (unsteady) flow, transient (unsteady) mass transport | Problem measure | 877.67 m |
| Time stepping scheme | Fully implicit with constant time steps | Number of layers | 29 |
| Upwinding | Full up winding | Number of slices | 30 |
| Number of time steps | 100 | Type | Saturated |
| Length of time step | $3.65 \cdot 10^4$ d | Dimension | Three-dimensional |
| Error tolerance | $1 \cdot 10^{-2}$ applied to Euclidian $L_2$ integral (RMS) norm | Element type | 6-noded triangular prism |
| Maximum number of iterations per time step | 12 | Mesh elements | 224228 |
| Adaptive mesh error | $1 \cdot 10^{-2}$ | Mesh nodes | 119010 |
| A posteriori error estimator | Onate–Bugeda algorithm | Mesh optimization | Not done |
| Velocity approximation | Improved consistent velocity approximation (by Frolkovic–Knabner algorithm) applied to linear elements with local smoothing | Aquifers | Unconfined (phreatic); other aquifers are Unspecified (automatically adapted) |
| Form of transport equation | Convective | Projection | None (3D with free surface) |
| Solver | Iterative equation solver | Adsorption law | Henry isotherm |

## DISCRETIZATION, PARAMETERIZATION, INITIAL AND BOUNDARY CONDITIONS

The flow in all aquifers in the numerical model is attributed to 29 layers (30 slices) and is represented by a 3D finite--element grid of 224228 mesh elements (Fig. 3).

The geometrical discretization (Fig. 3) of the model and model parameters values are based on data presented in Fig. 1 and Table 1. The discretization of the model in terms of boundary conditions is shown in Fig. 3 and Tables 4, 5.

For the numerical model, the layers are adjusted to the geometry of lithological bodies. In the first simple model approach, the parameters are assumed to be constant within the whole modeling domain; e. g., each layer consists of one zone. In the final approach, three zones with different parameters were selected. For a brief illustration of groundwater flow modeling features, a modeled hydraulic head distribution in the 16th modelling layer is given, which corresponds to pumping the Ordovician–Cambrian aquifer (Fig. 4).

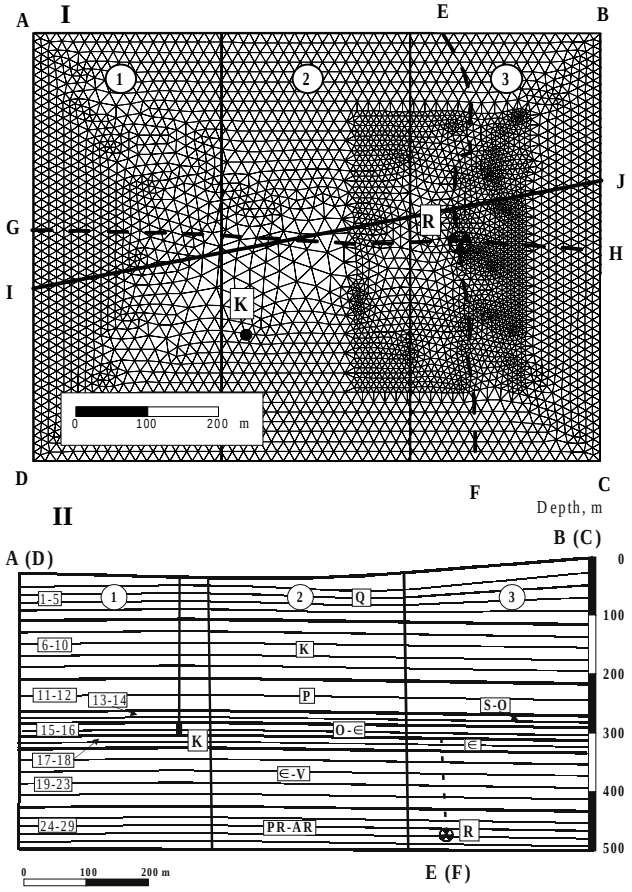


**Fig. 3.** Finite-element grid used for the model domain of South-eastern Lithuania (see Table 4): I – plan view, II – cross-section IJ: *1–3* – zones with different parameter values, AD and BC impervious boundaries, AB and CD – pervious boundaries, EF and GH – perpendicular single fractures, IJ – line of modeled cross-section, R – location of repository, K – pumping well installed in Ordovician–Cambrian aquifer

**3 pav.** Radionuklidų pernašos vandeninguosiuose horizontuose Pietryčių Lietuvos sąlygomis modelio baigtinių elementų tinklelis (žr. 4 lentelę): I – plane, II – pjūvyje IJ: *1–3* skirtingų parametrų zonos, AD ir BC – laidžios modelio ribos, AB ir CD – nelaidžios (šoninės) modelio ribos, EF ir GH – tektoniniai lūžiai, IJ – modelio pjūvio linija, R – saugyklos vieta, K – eksploatacinis gręžinys ordoviko–kambro vandeningajame komplekse

## MODEL CALIBRATION AND SENSITIVITY ANALYSES

Model calibration by many repeated runs is routine in numerical simulation (Hoteit, Firoozabadi, 2005; Samper--Calvete, Garsia-Vera, 1998). Model calibration in this study is a process by which the structure and parameters of a numerical model are progressively changed in an iterative manner to obtain an acceptable match between observed or expected and computed hydraulic heads and departing as little as possible from the original conceptual model. In addition to fitting hydraulic heads, calibration was based on the following criteria: computed water levels should always stand below the topographic surface; estimated hydraulic conductivities should be consistent with conductivities derived from available hydrogeological data; spatial patterns of parameters should be consistent with available geological information. A model of direct experimental data for substantiation of mass transport is impossible, because tracer experiments with long-living mobile radionuclides (I-129) are hardly validated, and the process of large--scale radionuclide transport is very long-lasting.

Parameters of relevance under far-field flow conditions routinely include hydraulic conductivity ($K$), areal recharge, hydraulic heads ($h$) specified along boundaries, dispersivity parameters ($\beta_L$, $\beta_T$). Areal

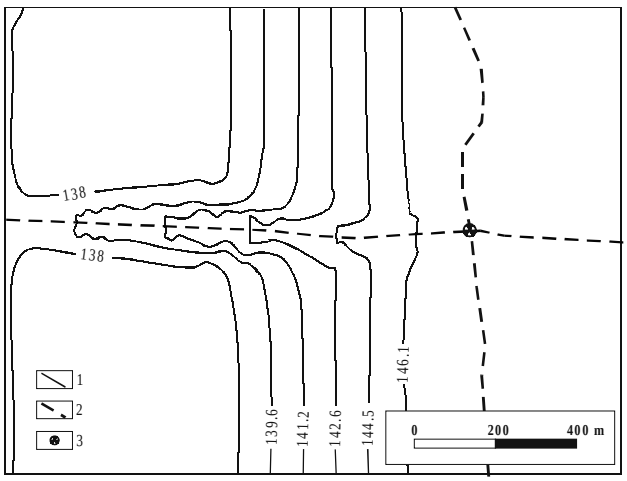


**Fig. 4.** Simulated hydraulic head of 27th layer representing Proterozoic–Archaean aquifer after 10 000 years: *1* – isoline of hydraulic head, m a. s. l., *2* – tectonic fault, *3* – repository

**4 pav.** Proterozojaus–Archėjaus vandeningojo horizonto hidraulinio spūdžio modelis po 10000 metų: *1* – spūdžio izolinija m abs. a., *2* – tektoninis lūžis, *3* – saugykla

Table 4. **Flow boundary conditions for the model domain of Southern Lithuania after model calibration (Fig. 3)**
4 lentelė. **Požeminio vandens tėkmių modelio, skirto Pietų Lietuvos hidrogeologinei būklei, ribinės sąlygos po modelio kalibracijos (3 pav.)**

| Section or point (slice) | Type | Value | Comment |
|---|---|---|---|
| A-B (1-30) | - | - | Unspecified (impervious) for all 30 slices |
| B-C (1-30) | Dirichlet (1st kind) | $h_1$=155 m; $h_2$=154.8 m; $h_3$=154.6 m; $h_4$=154.4 m; $h_5$=155.2 m; $h_6$=154 m; $h_7$=153.8 m; $h_8$=153.6 m; $h_9$=153.4 m; $h_{10}$=153.2 m; $h_{11}$=153 m; $h_{12}$=152.5 m; $h_{13}$=152 m; $h_{14}$=151.5 m; $h_{15}$=151 m; $h_{16}$=150.5 m; $h_{17}$=150 m; $h_{18}$=149.5 m; $h_{19}$=149 m; $h_{20}$=148.8 m; $h_{21}$=148.6 m; $h_{22}$=148.4 m; $h_{23}$=148.2 m; $h_{24}$=148 m; $h_{25}$=147.6 m; $h_{26}$=147.2 m; $h_{27}$=146.8 m; $h_{28}$=146.4 m; $h_{29}$=146 m; $h_{30}$=145.5 m | Pervious boundary (influx) |
| C-D (1-30) | - | - | Unspecified (impervious) for all 30 slices |
| D-A (1-30) | Dirichlet (1st kind) | $h_1$=130 m; $h_2$=130.2 m; $h_3$=130.4 m; $h_4$=130.6 m; $h_5$=130.8 m; $h_6$=131 m; $h_7$=131.2 m; $h_8$=131.4 m; $h_9$=131.6 m; $h_{10}$=131.8 m; $h_{11}$=132 m; $h_{12}$=132.5 m; $h_{13}$=133 m; $h_{14}$=133.5 m; $h_{15}$=134 m; $h_{16}$=134.5 m; $h_{17}$=135 m; $h_{18}$=135.5 m; $h_{19}$=136 m; $h_{20}$=136.2 m; $h_{21}$=136.4 m; $h_{22}$=136.6 m; $h_{23}$=136.8 m; $h_{24}$=137 m; $h_{25}$=137.4 m; $h_{26}$=137.8 m; $h_{27}$=138.2 m; $h_{28}$=138.6 m; $h_{29}$=139 m; $h_{30}$=139.5 m | Pervious boundary (outflow) |
| E-F (19-30) | Dirichlet (1st kind) | $h_{19-30}$=147 m | Pervious boundary (influx into fractures representing tectonic fault zone) |
| K (17) | (4th kind) | $Q_\rho^w$=3000 m³/d | Pumping rate of single well |

Table 5. **Boundary conditions of contaminant mass transport for the convective form**
5 lentelė. **Radionuklidų (masės) pernašos ribinės sąlygos esant konvekcinei transporto lygties formai**

| Point (layer) | Type | Value | | Comment |
|---|---|---|---|---|
| | | years | Bq/l | |
| R | Dirichlet | <10000 | 0 | Release from repository |
| (27) | (1st kind); time-varying function $C(x_i,t)=C_1^R(t)$ | 10000–100000 | $8.7\cdot10^{-4}$ | (defected canister) to the receiving triangular cell with the area of 19.4 m² |
| | | 100000–200000 | $8.7\cdot10^{-5}$ | |
| | | 200000–300000 | $8.7\cdot10^{-7}$ | |
| | | 300000–400000 | $4.3\cdot10^{-7}$ | |
| | | >400000 | 0 | |

recharge was assumed to be uniform throughout the study area ($1.4 \cdot 10^{-4}$ m/d).

A sensitivity analysis was performed in order to (a) quantify the uncertainty in the estimated parameters and of the parameters that remained fixed during calibration, and (b) evaluate the effect of some hypotheses of the conceptual model (for example, the influence of one transverse fracture, of two perpendicular fractures and of pumping well). Sensitivity analysis was carried out using two structures of the model: (a) with one transverse fracture, and (b) with two perpendicular fractures. The sensitivity of the model was tested for hydraulic conductivities of all layers and for fracture porosity in the crystalline basement.

For sensitivity analysis, runs of the model were made for three sets of hydraulic conductivity: 1 – normal hydraulic conductivity corresponding to values of Table 1; 2 – normal conductivity increased by one order of magnitude; 3 – normal conductivity decreased by one order of magnitude. The change of the volumetric activity of I-129 in groundwater for a period of 0 to $10^6$ years was reconstructed in the pumping well (16th layer – Ordovician–Cambrian aquifer, about 363 m from the repository).

For one transverse fracture model, the volumetric activity of I-129 in groundwater at the pumping well did not differ by more than two orders of magnitude for sensitivity runs throughout the whole modeled period. The I-129 activity was highest when the normal conductivity decreased by one order of magnitude. The peak activity value in all cases did not exceed $10^{-4}$ Bq/l. The peak activity value of I-129 for the case when the normal conductivity increased by one order of magnitude was close to $10^{-6}$ Bq/l (Fig. 5).

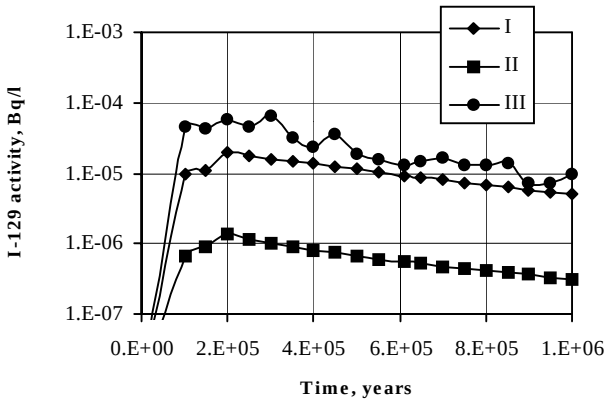


**Fig. 5.** Computed temporal distributions of I-129 activity in groundwater from pumping well for model case of single transverse fracture with different sets of hydraulic conductivity values (I – normal hydraulic conductivity; II – normal conductivity increased by one order of magnitude; III – normal conductivity decreased by one order of magnitude)

**5 pav.** Modelio su vienu skersiniu tektoniniu lūžiu I-129 aktyvumo kaita eksploatuojamo vandeningojo komplekso vandenyje esant skirtingiems parametrų rinkiniams (I – bazinis filtracijos koeficiento reikšmių rinkinys, II – atvejis, kai filtracijos koeficiento reikšmės dešimt kartų didesnės nei baziniame rinkinyje, III – atvejis, kai filtracijos koeficiento reikšmės dešimt kartų mažesnės nei baziniame rinkinyje)

For the two perpendicular fractures model, the volumetric activity of I-129 in groundwater at the pumping well and in the point zone closer to release was very similar for all sensitivity runs throughout the whole modeled period. Namely, the highest I-129 activity in groundwater at the pumping well varied within $10^{-8}$–$10^{-11}$ Bq/l and closer to the release point zone within $10^{-3}$-$10^{-5}$ Bq/l. The calibrated model was less sensitive to changes in hydraulic conductivity parameters over the whole domain due to the prevailing groundwater flow through a significantly more permeable longitudinal fracture.

For sensitivity analysis of the fracture zone, porosity two runs of the model were performed: 1 – when the porosity of the fracture zone was assumed to be 0.3, 2 – when the porosity of the fracture zone was assumed to be 0.03. The main findings of the analysis were the following: at a lower porosity value the activity concentration of I-129 in groundwater at the pumping well was by one order of magnitude lower compared to the case with a higher value of porosity, while the activity concentration of I-129 in the longitudinal fracture was approximately the same in both cases; however, the time of contamination plume spreading in the longitudinal fracture was shorter in case of a lower porosity.

## SPATIAL DISTRIBUTION OF ONTAMINATION PLUME

The FEFLOW computer program enables spatial and temporal analysis of modelling results in many ways. For demonstration, we present here the calculation results for contamination plume at a moment when the peak activity of I-129 is expected. This is the time of approximately 10 000 years after the initial moment of release. Yet the initial moment of release will occur 200 000 years following the repository closure. Thus, the migration of the most mobile radionuclide I-129 in groundwater will be possible only in a very remote future for the normal evolution scenario.

Calculation results for the section show that the contamination plume of $10^{-7}$ Bq/l does not reach farther than 700 m from the defected canister and includes the Cambrian–Vendian and weathered Proterozoic–Archaean aquifers (Fig. 6).

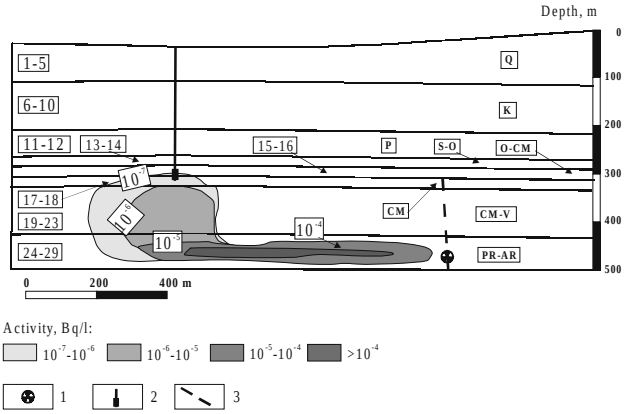


**Fig. 6.** Predicted contamination plume of I-129 (cross-section line IJ in Fig. 3) after 10 000 years: *1* – repository, *2* – pumping well, *3* – tectonic fault

**6 pav.** Prognozuojamas I-129 pasiskirstymas požeminiame vandenyje (pjūvio linija IJ žr. 3 pav.) po 10 000 metų: *1* – saugykla, *2* – eksploatacinis gręžinys, *3* – tektoninis lūžis

Imitation of discharge conditions showed that the groundwater containing I-129 with activity concentration of $10^{-7}$ Bq/l or less is able to reach the productive well or earth surface.

The areal distribution pattern of activity concentration of I-129 in the most highly polluted water of the Proterozoic–Archaean aquifer is shown Fig. 7.

The highest predicted value of activity in the zone of longitudinal single fracture is of the order $10^{-4}$ Bq/l. Contamination plume of $10^{-4}$ Bq/l reaches the observation point near the defected canister (90 m), whereas groundwater containing I-129 with activity concentration of $10^{-4}$-$10^{-7}$ Bq/l discharges out of the longitudinal fracture outside the model boundaries in the flow direction.

The I-129 activity concentration corresponding to the dose limit of 1 mSv/year for drinking water pathway is 27.5 Bq/l. Yet today, for example, the globally predicted level of I-129 activity in the river water is about $10^{-6}$ Bq/l.

The numerical model should be improved in the future, and more scenarios of long-term evolution for repository-surrounded media should be worked out.

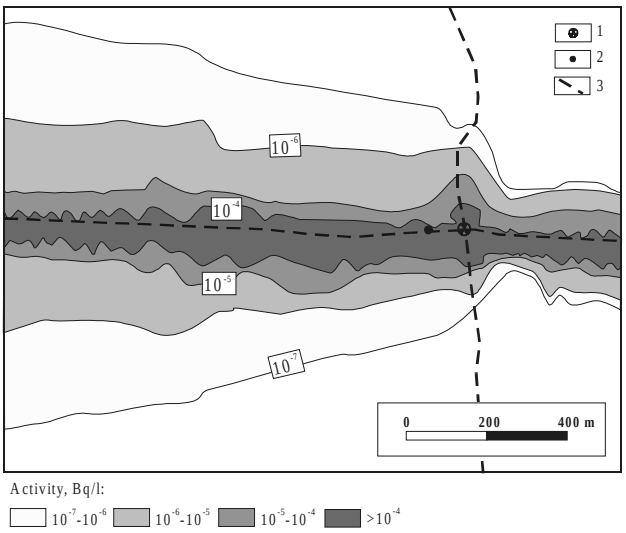


**Fig. 7.** Predicted contamination plume of I-129 in Preoterozoic–Archaean aquifer after 10 000 years: *1* – repository, *2* – observation point, *3* – tectonic fault
**7 pav.** Prognozuojamas I-129 pasiskirstymas Proterozojaus–Archėjaus vandeningajame horizonte po 10 000 metų: *1* – saugykla, *2* – stebimasis gręžinys, *3* – tektoninis lūžis

## CONCLUSIONS

The crystalline basement is the best worldwide investigated medium in connection with disposal of spent nuclear fuel. In Lithuania, thick sedimentary layers of varying origin and properties cover the crystalline basement. Complex structures of overlying layers make performance assessment significantly more sophisticated and complicated.

Modeling of most safety-relevant radionuclide I-129 migration for a tectonically fractured domain shows that doses to humans even in such case will not exceed the existing dose restrictions. Based on worldwide experience, it would in principle be possible to dispose of spent nuclear fuel and other long-lived high-level radioactive wastes in a repository built in the crystalline basement.

## ACKNOWLEDGEMENTS

The Lithuanian State Science and Studies Foundation funded this study within the frame of the program "Research and development in the field of radwaste generation, migration and impact on the environment and human health – RASSA" (contract no. C-19/2004). Partial support was given by RATA. The authors are grateful to Prof. A. Poškas and Ph. D. student A. Brazauskaitė from LEI, R. Kanopienė from LGT, Prof. I. Neretnieks, Assist. Prof. L. Moreno and Dr. J. Crawford from KTH – Royal Institute of Technology (Stockholm, Sweden) for assistance and co-operation. Special thanks belong to reviewers Prof. A. Kudelsky (Institute of Geochemistry and Geophysics of the NAS of Belarus, Minsk), Prof. R. Mokrik (Vilnius University) and Dr. S. Motiejūnas (RATA), whose comments resulted in a significantly improved manuscript.

### References

Adam Ch., Petschel M., Koerner W. 1985. Empfehlungen zur hydrogeologischen Begutachtung der Standorte von Kernanlagen im Rahmen des Strahlenschutz-Genehmigungsverfahrens. 25–27.

Baker A. J. 1998. Finite element method. R. W. Johnson (ed.). The handbook of fluid dynamics, Chapter 28. CRC Press, Springer.

Brazauskaitė A., Poškas P. 2005. Radionuklidų sklaida iš kristalinėse uolienose įrengto geologinio kapinyno RBMK-1500 panaudotam branduoliniam kurui laidoti. 1. Kapinyno koncepcija. *Energetika.* Vilnius. ***3***. 70–78.

Chang S. H., Cho W. J. 1984. Risk analysis of radioactive waste repository based on the time-dependent hazard rate. *Radioactive Waste Management and the Nuclear Fuel Cycle*. ***5****(1)*, 63–80.

Chavent G., Jaffe J. 1986. Mathematical models and finite elements for reservoir simulation. New York, North Holland.

Concept of repository in crystalline rocks. 2005. *Investigations of possibilities to dispose of spent nuclear fuel in Lithuania: a model case*. Vilnius, RATA, LEI, LGT and SKB Report. ***2***. 28.

De Marsily G., Gonçalvès J., Violette S., Castro M.-C. 2002. Migration mechanisms of radionuclide from a clay repository toward adjacent aquifers and the surface. *Applied Physics*. ***3***. 945–956.

Deep repository for spent nuclear fuel. SKB Technical Report TR-99-06. Main Report. 1998.

Diersch H.-J. 2002. Wasy Software FEFLOW. Finite Element Subsurface Flow and Transport Simulation System: Reference Manual. Wasy Institute for Water Resources Planning and Systems Research Ltd. Berlin, Germany.

Dundulis K., Gadeikis S., Ignatavičius V. 2004. Kvartero nuogulų inžinerinių geologinių sąlygų formavimasis. *Lietuvos žemės gelmių raida ir ištekliai*. Vilnius. 320–330.

Ferziger J. H., Peric M. 1996. Computational methods for fluid dynamics. Springer, Berlin.

Generic safety assessment of repository in crystalline rocks. 2005. *Investigations of possibilities to dispose of spent nuclear fuel in Lithuania: a model case*. RATA, LEI, LGT and SKB Report. ***3***. 54.

Hoteit H., Firoozabadi A. 2005. Multicomponent fluid flow by discontinuous Galerkin and mixed methods in unfractured and fractured media. *Water Resour. Res.* ***41***. W11412, doi: 10.1029/2005WR004339. 15.

IAEA Deep Underground Disposal of Radioactive Waste: Near-Field Effects. 1985. *Technical reports series No. 251*. IAEA. Vienna. 60.

Krishnamoorthy T.M., Nair R.N. 1994. Groundwater models for safety analysis of low-level radioactive waste repositories. *Nuclear Geophysics*. ***8****(4)*. 351–360.

Lucero D. A. 1998. Laboratory Column Experiments for Radionuclide Adsorption Studies of the Culebra Dolomite

Member of the Rustler Formation SAND97-1763. Sandia National Laboratories, Albuquerque.

Mikšys R. B. 2004. Ikikvartero sluoksnių uolienų fizikinių ir geomechaninių savybių formavimosi ypatybės. *Lietuvos žemės gelmių raida ir ištekliai*. Vilnius. 313–317.

Mokrik R. 2003. Baltijos baseino paleohidrogeologija. *Neoproterozojus ir fanerozojus*. Vilnius.

Paškevičius J. 1994. Baltijos respublikų geologija. Vilnius.

Samper-Calvete F. J., García-Vera M. A. 1998. Inverse modelling of groundwater flow in the semiarid evaporitic closed basin of Los Monegros, Spain. *Hydrogeology Journal*. ***6(1)***. 33–49.

Suitability of geological environment in Lithuania for disposal of spent nuclear fuel. 2005. *Investigations of possibilities to dispose of spent nuclear fuel in Lithuania: a model case.* Vilnius, RATA, LEI, LGT and SKB Report. ***1.*** 51–60.

Summary report of work done during Basic Design. KBS-3, SKB Report R-04-42. Stockholm, 2004.

The scientific and regulatory basis for the geological disposal of radioactive waste. D. Savage (ed.). 1995. Chichester–New York–Brisbane–Toronto–Singapure.

Vieno T. 1994. Safety Analysis of Disposal of Spent Nuclear Fuel. Technical research center of Finland, ESPOO.

Vilks P., Caron F., Haas M. K. 1998. Potential for the formation and migration of colloidal material from a near surface waste disposal site. *Applied Geochemistry*. ***13***. 31–42.

Иодказис В. И. 1989. Региональная гидрогеология Прибалтики. Вильнюс: Мокслас. 38–176 с.

**Vaidotė Jakimavičiūtė-Maselienė, Jonas Mažeika, Rimantas Petrošius**

## RADIONUKLIDŲ PERNAŠOS KRISTALINIAME PAMATE MODELIAVIMAS PANAUDOTO BRANDUOLINIO KURO LAIDOJIMO GALIMYBEI PADEMONSTRUOTI (PIETRYČIŲ LIETUVOS PAVYZDYS)

Santrauka

Pagal radioaktyviųjų atliekų tvarkymo strategiją, kaip viena iš alternatyvų Lietuvoje yra numatoma galimybė panaudotą branduolinį kurą ir ilgaamžes radioaktyviąsias atliekas, susidarančias Ignalinos AE, laidoti giliose geologinėse formacijose. Pradiniai 2001–2004 m. tyrimai buvo skirti šiam tikslui parinkti potencialiai tinkančias geologines formacijas. Dėl didelio anksčiau atliktų tyrimų duomenų kiekio modeliui sudaryti buvo pasirinktas kristalinis pamatas. Požeminio vandens tėkmių ir radionuklido (itin mobilaus ir ilgaamžio jodo-129) pernaša modeliuota kompiuterine programa FEFLOW, įvertinant normalios raidos hipotezę (Švedijos ekspertų pasiūlytas bei LEI specialistų apskaičiuotas kanistro defekto scenarijus) bei modelinį 0,8 km ilgio, 0,6 km pločio ir 0,52 km gylio tolimojo lauko bloką. Modelinis blokas atspindi Pietryčių Lietuvai būdingas hidrogeologines sąlygas. Darbo metu buvo modeliuotas atvejis, kai per tektoniškai suardytą zoną, kurioje yra patalpintas pažeistas kanistras, požeminio vandens tėkmės srūva į žemės paviršių. Pagrindiniai skaičiavimų rezultatai: didžiausias tikėtinas I-129 tūrinis aktyvumas požeminiame tektoniškai suardytos zonos vandenyje šalia kanistro neviršys $10^{-4}$ Bq/l, požeminio vandens aktyvios apykaitos zonoje bus apie $10^{-7}$ Bq/l. Jei žmogus gertų tokį požeminį vandenį, jo gauta efektinė apšvitos dozė neturėtų pasiekti dozės ribos (1 mSv per metus).

**Вайдоте Якимавичюте-Масялене, Йонас Мажейка, Римантас Пятрошюс**

## МОДЕЛИРОВАНИЕ ПЕРЕНОСА РАДИОНУКЛИДОВ В КРИСТАЛЛИЧЕСКОМ ФУНДАМЕНТЕ В ЦЕЛЯХ ДЕМОНСТРАЦИИ ВОЗМОЖНОСТИ ЗАХОРОНЕНИЯ ОТРАБОТАННОГО ЯДЕРНОГО ТОПЛИВА (НА ПРИМЕРЕ ЮГО-ВОСТОЧНОЙ ЛИТВЫ)

Резюме

Стратегия обращения с радиоактивными отходами Литвы как одну из альтернатив предусматривает оценку возможности захоронения отработанного ядерного топлива и долгоживущих радиоактивных отходов в глубокие геологические формации. Начальная оценка пригодности всех потенциальных геологических формаций для захоронения отработанного ядерного топлива выполнена в Литве в течение 2001–2004 гг. Из-за большого объема существующей разносторонней информации кристаллический фундамент был отобран в первую очередь для моделирования потоков подземных вод и переноса радионуклидов.

Принимая во внимание главные предпосылки нормального развития (шведскими экспертами предложенный и экспертами Литовского энергетического института оцененный сценарий дефектного канистра с отработанным ядерным топливом) и подобранные параметры, характерные для кристаллического фунда-мента и вышележащей толщи осадочных пород южной части Литвы ($0{,}8 \times 0{,}6 \times 0{,}52$-километровый блок дальнего поля) моделировался перенос радионуклидов (иода-129 как мобильного и долгоживущего радио-нуклида) с потоком подземных вод, используя компьютерный код FEFLOW. Через дефектный канистр, гипотетически расположенный в тектонически нарушенной зоне, средствами моделирования был воссоздан восходящий поток подземных вод.

Главные результаты численного моделирования следующие: в случае восходящего потока подземных вод максимум активности I-129 в воде тектонически нарушенной зоны рядом с дефектным канистром не будет превышать $10^{-4}$ Бк/л, а в зоне активного водообмена – близок к $10^{-7}$ Бк/л. Результаты показы-вают, что человеком через питьевую воду полученные дозы должны быть ниже предела дозы (1 мЗв/год).